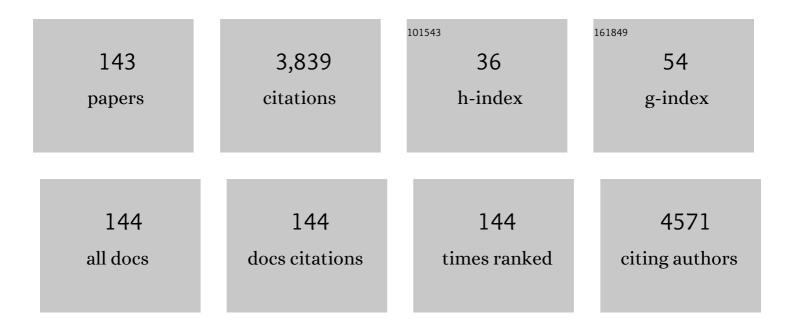


List of Publications by Year in descending order

Source: https://exaly.com/author-pdf/891938/publications.pdf Version: 2024-02-01



Curoli

#	Article	IF	CITATIONS
1	Lipase-catalysed direct Mannich reaction in water: utilization of biocatalytic promiscuity for C–C bond formation in a "one-pot―synthesis. Green Chemistry, 2009, 11, 777.	9.0	167
2	Chemical indices (CIA and WIP) as proxies for integrated chemical weathering in China: Inferences from analysis of fluvial sediments. Sedimentary Geology, 2012, 265-266, 110-120.	2.1	156
3	Changes in Annual Extremes of Daily Temperature and Precipitation in CMIP6 Models. Journal of Climate, 2021, 34, 3441-3460.	3.2	132
4	Molecular mechanisms and in vitro antioxidant effects of Lactobacillus plantarum MA2. Food Chemistry, 2017, 221, 1642-1649.	8.2	112
5	Charge-Transfer Induced High Efficient Hydrogen Evolution of MoS2/graphene Cocatalyst. Scientific Reports, 2015, 5, 18730.	3.3	105
6	Improving anaerobic fermentation of waste activated sludge using iron activated persulfate treatment. Bioresource Technology, 2018, 268, 68-76.	9.6	98
7	Revisiting the effects of hydrodynamic sorting and sedimentary recycling on chemical weathering indices. Geochimica Et Cosmochimica Acta, 2018, 227, 48-63.	3.9	97
8	Kuroshio subsurface water feeds the wintertime Taiwan Warm Current on the inner East China Sea shelf. Journal of Geophysical Research: Oceans, 2016, 121, 4790-4803.	2.6	85
9	Provenance weathering and erosion records in southern Okinawa Trough sediments since 28 ka: Geochemical and Sr–Nd–Pb isotopic evidences. Chemical Geology, 2016, 425, 93-109.	3.3	85
10	Lipase-catalysed decarboxylative aldol reaction and decarboxylative Knoevenagel reaction. Green Chemistry, 2009, 11, 1933.	9.0	80
11	Facile synthesis of the Basolite F300-like nanoscale Fe-BTC framework and its lithium storage properties. RSC Advances, 2016, 6, 114483-114490.	3.6	79
12	Joint bias correction of temperature and precipitation in climate model simulations. Journal of Geophysical Research D: Atmospheres, 2014, 119, 13,153.	3.3	76
13	Larger Increases in More Extreme Local Precipitation Events as Climate Warms. Geophysical Research Letters, 2019, 46, 6885-6891.	4.0	76
14	Detrital zircon geochronology of river sands from Taiwan: Implications for sedimentary provenance of Taiwan and its source link with the east China mainland. Earth-Science Reviews, 2017, 164, 31-47.	9.1	60
15	Geochemistry of riverâ€borne clays entering the <scp>E</scp> ast <scp>C</scp> hina <scp>S</scp> ea indicates two contrasting types of weathering and sediment transport processes. Geochemistry, Geophysics, Geosystems, 2015, 16, 3034-3052.	2.5	58
16	Three Gorges Dam alters the Changjiang (Yangtze) river water cycle in the dry seasons: Evidence from H-O isotopes. Science of the Total Environment, 2016, 562, 89-97.	8.0	58
17	How Much Information Is Required to Well Constrain Local Estimates of Future Precipitation Extremes?. Earth's Future, 2019, 7, 11-24.	6.3	55
18	Endolysin, a Promising Solution against Antimicrobial Resistance. Antibiotics, 2021, 10, 1277.	3.7	55

#	Article	IF	CITATIONS
19	Promiscuous protease-catalyzed aldol reactions: A facile biocatalytic protocol for carbon–carbon bond formation in aqueous media. Journal of Biotechnology, 2010, 150, 539-545.	3.8	53
20	Preparation of hollow microsphere@onion-like solid nanosphere MoS ₂ coated by a carbon shell as a stable anode for optimized lithium storage. Nanoscale, 2016, 8, 420-430.	5.6	53
21	Biomimetic Dendrimer–Peptide Conjugates for Early Multiâ€Target Therapy of Alzheimer's Disease by Inflammatory Microenvironment Modulation. Advanced Materials, 2021, 33, e2100746.	21.0	50
22	Provenance study of the Holocene sediments in the Changjiang (Yangtze River) estuary and inner shelf of the East China sea. Quaternary International, 2017, 441, 147-161.	1.5	49
23	The recovery of Zn and Pb and the manufacture of lightweight bricks from zinc smelting slag and clay. Journal of Hazardous Materials, 2014, 271, 220-227.	12.4	48
24	Major sinks of the Changjiang (Yangtze River)-derived sediments in the East China Sea during the late Quaternary. Geological Society Special Publication, 2016, 429, 137-152.	1.3	46
25	Efficient production of short-chain fatty acids from anaerobic fermentation of liquor wastewater and waste activated sludge by breaking the restrictions of low bioavailable substrates and microbial activity. Bioresource Technology, 2018, 268, 549-557.	9.6	46
26	Silica-assisted cross-linked polymer electrolyte membrane with high electrochemical stability for lithium-ion batteries. Journal of Colloid and Interface Science, 2021, 594, 1-8.	9.4	45
27	Study on anaerobic ammonium oxidation process coupled with denitrification microbial fuel cells (MFCs) and its microbial community analysis. Bioresource Technology, 2015, 175, 545-552.	9.6	44
28	The time scale of river sediment source-to-sink processes in East Asia. Chemical Geology, 2016, 446, 138-146.	3.3	43
29	Novel dual-petal nanostructured WS ₂ @MoS ₂ with enhanced photocatalytic performance and a comprehensive first-principles investigation. Journal of Materials Chemistry A, 2015, 3, 20225-20235.	10.3	41
30	Ecotoxicity and environmental fates of newly recognized contaminants-artificial sweeteners: A review. Science of the Total Environment, 2019, 653, 1149-1160.	8.0	41
31	Damming effect on the Changjiang (Yangtze River) river water cycle based on stable hydrogen and oxygen isotopic records. Journal of Geochemical Exploration, 2016, 165, 125-133.	3.2	40
32	Contribution of Global warming and Urbanization to Changes in Temperature Extremes in Eastern China. Geophysical Research Letters, 2019, 46, 11426-11434.	4.0	40
33	How Do Biocides That Occur in Waste Activated Sludge Affect the Resource Recovery for Short-Chain Fatty Acids Production. ACS Sustainable Chemistry and Engineering, 2019, 7, 1648-1657.	6.7	40
34	Rapid Warming in Summer Wet Bulb Globe Temperature in China with Human-Induced Climate Change. Journal of Climate, 2020, 33, 5697-5711.	3.2	40
35	Rational design of porous Sn nanospheres/N-doped carbon nanofibers as an ultra-stable potassium-ion battery anode material. Journal of Materials Chemistry A, 2021, 9, 5740-5750.	10.3	40
36	Synthesis and catalysis of Ag nanoparticles trapped into temperature-sensitive and conductive polymers. Journal of Materials Science, 2014, 49, 6872-6882.	3.7	39

#	Article	IF	CITATIONS
37	A probabilistic assessment of the likelihood of vegetation drought under varying climate conditions across China. Scientific Reports, 2016, 6, 35105.	3.3	39
38	Evaluation of Temperature and Precipitation Simulations in CMIP6 Models Over the Tibetan Plateau. Earth and Space Science, 2021, 8, e2020EA001620.	2.6	39
39	Antioxidative effects in vivo and colonization of Lactobacillus plantarum MA2 in the murine intestinal tract. Applied Microbiology and Biotechnology, 2016, 100, 7193-7202.	3.6	38
40	Bisphenol a electrochemical sensor based on multi-walled carbon nanotubes/polythiophene/Pt nanocomposites modified electrode. Analytical Methods, 2016, 8, 3333-3338.	2.7	37
41	Recent Very Hot Summers in Northern Hemispheric Land Areas Measured by Wet Bulb Globe Temperature Will Be the Norm Within 20 Years. Earth's Future, 2017, 5, 1203-1216.	6.3	37
42	Astaxanthin and its gold nanoparticles mitigate cadmium toxicity in rice by inhibiting cadmium translocation and uptake. Science of the Total Environment, 2021, 786, 147496.	8.0	37
43	A Facile Surfactant-Assisted Reflux Method for the Synthesis of Single-Crystalline Sb ₂ Te ₃ Nanostructures with Enhanced Thermoelectric Performance. ACS Applied Materials & Interfaces, 2015, 7, 14263-14271.	8.0	36
44	Probiotic Properties and Cellular Antioxidant Activity of Lactobacillus plantarum MA2 Isolated from Tibetan Kefir Grains. Probiotics and Antimicrobial Proteins, 2018, 10, 523-533.	3.9	34
45	Promoting the anaerobic production of short-chain fatty acids from food wastes driven by the reuse of linear alkylbenzene sulphonates-enriched laundry wastewater. Bioresource Technology, 2019, 282, 301-309.	9.6	34
46	H. pylori CagA activates the NLRP3 inflammasome to promote gastric cancer cell migration and invasion. Inflammation Research, 2022, 71, 141-155.	4.0	34
47	Comparative genomics of Lactobacillus kefiranofaciens ZW3 and related members of Lactobacillus. spp reveal adaptations to dairy and gut environments. Scientific Reports, 2017, 7, 12827.	3.3	33
48	PVP-capped silver nanoparticles as catalysts for polymerization of alkylsilanes to siloxane composite microspheres. Journal of Materials Chemistry, 2006, 16, 3606.	6.7	30
49	Review on the determination and distribution patterns of a widespread contaminant artificial sweetener in the environment. Environmental Science and Pollution Research, 2019, 26, 19078-19096.	5.3	30
50	Fucoidan from sea cucumber Holothuria polii: Structural elucidation and stimulation of hematopoietic activity. International Journal of Biological Macromolecules, 2020, 154, 1123-1131.	7.5	29
51	BAG3 is upregulated by c-Jun and stabilizes JunD. Biochimica Et Biophysica Acta - Molecular Cell Research, 2013, 1833, 3346-3354.	4.1	28
52	Synthesis of open helmet-like carbon skeletons for application in lithium-ion batteries. Journal of Materials Chemistry A, 2018, 6, 3877-3883.	10.3	28
53	Detection of Human Influence on Precipitation Extremes in Asia. Journal of Climate, 2020, 33, 5293-5304.	3.2	26
54	Phytoplankton Blooms off a High Turbidity Estuary: A Case Study in the Changjiang River Estuary. Journal of Geophysical Research: Oceans, 2019, 124, 8036-8059.	2.6	25

#	Article	IF	CITATIONS
55	Deepwater redox changes in the southern Okinawa Trough since the last glacial maximum. Progress in Oceanography, 2015, 135, 77-90.	3.2	24
56	The response of sediment microbial communities to temporal and site-specific variations of pollution in interconnected aquaculture pond and ditch systems. Science of the Total Environment, 2022, 806, 150498.	8.0	24
57	Doubling the <i>ZT</i> record of TiS ₂ -based thermoelectrics by incorporation of ionized impurity scattering. Journal of Materials Chemistry C, 2018, 6, 9345-9353.	5.5	22
58	Absorption and Removal Efficiency of Low-Partial-Pressure H ₂ S in a Monoethanolamine-Activated <i>N</i> -Methyldiethanolamine Aqueous Solution. Energy & Fuels, 2019, 33, 629-635.	5.1	21
59	Two different fucosylated chondroitin sulfates: Structural elucidation, stimulating hematopoiesis and immune-enhancing effects. Carbohydrate Polymers, 2020, 230, 115698.	10.2	21
60	Sources and burial of organic carbon in the middle Okinawa Trough during late Quaternary paleoenvironmental change. Deep-Sea Research Part I: Oceanographic Research Papers, 2016, 118, 46-56.	1.4	20
61	Effects of Pore Structures of Different Maceral Compositions on Methane Adsorption and Diffusion in Anthracite. Applied Sciences (Switzerland), 2019, 9, 5130.	2.5	20
62	Catalytic ozonation treatment of papermaking wastewater by Ag-doped NiFe2O4: Performance and mechanism. Journal of Environmental Sciences, 2020, 97, 75-84.	6.1	20
63	A high-performance solid electrolyte assisted with hybrid biomaterials for lithium metal batteries. Journal of Colloid and Interface Science, 2022, 608, 313-321.	9.4	20
64	A facile method to prepare superhydrophobic nanocellulose-based aerogel with high thermal insulation performance via a two-step impregnation process. Cellulose, 2022, 29, 245-257.	4.9	20
65	Magnetic properties of sediments from major rivers, aeolian dust, loess soil and desert in China. Journal of Asian Earth Sciences, 2012, 45, 190-200.	2.3	19
66	Short-term Pharmacological Inhibition of MyD88 Homodimerization by a Novel Inhibitor Promotes Robust Allograft Tolerance in Mouse Cardiac and Skin Transplantation. Transplantation, 2017, 101, 284-293.	1.0	19
67	Widespread persistent changes to temperature extremes occurred earlier than predicted. Scientific Reports, 2018, 8, 1007.	3.3	19
68	Decreased takeoff performance of aircraft due to climate change. Climatic Change, 2018, 151, 463-472.	3.6	19
69	Iridium-Catalyzed Alkylation of Amine and Nitrobenzene with Alcohol to Tertiary Amine under Base- and Solvent-Free Conditions. Journal of Organic Chemistry, 2019, 84, 2158-2168.	3.2	19
70	The Influence of Micro-Oxygen Addition on Desulfurization Performance and Microbial Communities during Waste-Activated Sludge Digestion in a Rusty Scrap Iron-Loaded Anaerobic Digester. Energies, 2017, 10, 258.	3.1	17
71	Pacific decadal oscillation impact on East China precipitation and its imprint in new geological documents. Science China Earth Sciences, 2018, 61, 473-482.	5.2	15
72	Constraining the transport time of lithogenic sediments to the Okinawa Trough (East China Sea). Chemical Geology, 2016, 445, 199-207.	3.3	14

#	Article	IF	CITATIONS
73	Origin of the springtime South China Sea Warm Current in the southwestern Taiwan Strait: Evidence from seawater oxygen isotope. Science China Earth Sciences, 2020, 63, 1564-1576.	5.2	14
74	Facilitating biofilm formation of Pseudomonas aeruginosa via exogenous N-Acy-L-homoserine lactones stimulation: Regulation on the bacterial motility, adhesive ability and metabolic activity. Bioresource Technology, 2021, 341, 125727.	9.6	14
75	Pilot-scale study on nitrogen and aromatic compounds removal in printing and dyeing wastewater by reinforced hydrolysis-denitrification coupling process and its microbial community analysis. Environmental Science and Pollution Research, 2015, 22, 9483-9493.	5.3	13
76	Characterizing the free ammonia exposure to the nutrients removal in activated sludge systems. RSC Advances, 2017, 7, 55088-55097.	3.6	13
77	Dynamic Amplification of Subtropical Extreme Precipitation in a Warming Climate. Geophysical Research Letters, 2020, 47, e2020GL087200.	4.0	13
78	Response of MiRNA-22-3p and MiRNA-149-5p to Folate Deficiency and the Differential Regulation of MTHFR Expression in Normal and Cancerous Human Hepatocytes. PLoS ONE, 2017, 12, e0168049.	2.5	13
79	Microstructure evolution with composition ratio in self-assembled WO ₃ –BiVO ₄ hetero nanostructures for water splitting. Journal of Materials Research, 2017, 32, 2790-2799.	2.6	12
80	Facets Matching of Platinum and Ferric Oxide in Highly Efficient Catalyst Design for Low-Temperature CO Oxidation. ACS Applied Materials & Interfaces, 2018, 10, 15322-15327.	8.0	12
81	Adding Zero-Valent Iron to Enhance Electricity Generation during MFC Start-Up. International Journal of Environmental Research and Public Health, 2020, 17, 806.	2.6	12
82	Recent Progress on Lipid Intake and Chronic Kidney Disease. BioMed Research International, 2020, 2020, 1-11.	1.9	12
83	Warming alters juvenile carp effects on macrophytes resulting in a shift to turbid conditions in freshwater mesocosms. Journal of Applied Ecology, 2022, 59, 165-175.	4.0	12
84	Comparative analysis of microbial community between different cathode systems of microbial fuel cells for denitrification. Environmental Technology (United Kingdom), 2016, 37, 752-761.	2.2	11
85	Sediment recycling and indication of weathering proxies. Acta Geochimica, 2017, 36, 498-501.	1.7	11
86	A New Defect Pyrochlore Oxide Sn _{1.06} Nb ₂ O _{5.59} F _{0.97} : Synthesis, Noble Metal Hybrids, and Photocatalytic Applications. Inorganic Chemistry, 2018, 57, 6641-6647.	4.0	11
87	Coordination of Superconductive Fault Current Limiters With Zero-Sequence Current Protection of Transmission Lines. IEEE Transactions on Applied Superconductivity, 2014, 24, 1-5.	1.7	10
88	The polysaccharides from <i>Grifola frondosa</i> attenuate CCl ₄ -induced hepatic fibrosis in rats <i>via</i> the TGF-β/Smad signaling pathway. RSC Advances, 2019, 9, 33684-33692.	3.6	10
89	A review of comminution age method and its potential application in the East China Sea to constrain the time scale of sediment source-to-sink process. Journal of Ocean University of China, 2015, 14, 399-406.	1.2	9
90	Chemical speciation of iron in sediments from the Changjiang Estuary and East China Sea: Iron cycle and paleoenvironmental implications. Quaternary International, 2017, 452, 116-128.	1.5	9

#	Article	IF	CITATIONS
91	XB130, regulated by miRâ€203, miRâ€219, and miRâ€4782â€3p, mediates the proliferation and metastasis of nonâ€smallâ€cell lung cancer cells. Molecular Carcinogenesis, 2020, 59, 557-568.	2.7	9
92	A machine learningâ€based survival prediction model of high grade glioma by integration of clinical and doseâ€volume histogram parameters. Cancer Medicine, 2021, 10, 2774-2786.	2.8	9
93	Single-Channel Speech Enhancement Based on Adaptive Low-Rank Matrix Decomposition. IEEE Access, 2020, 8, 37066-37076.	4.2	8
94	Coal Petrology Effect on Nanopore Structure of Lignite: Case Study of No. 5 Coal Seam, Shengli Coalfield, Erlian Basin, China. Natural Resources Research, 2021, 30, 681-695.	4.7	8
95	Melatonin enhances metallic oxide nanoparticle stress tolerance in rice <i>via</i> inducing tetrapyrrole biosynthesis and amino acid metabolism. Environmental Science: Nano, 2021, 8, 2310-2323.	4.3	8
96	Seasonal variability of stable isotopes in the Changjiang (Yangtze) river water and its implications for natural climate and anthropogenic impacts. Environmental Sciences Europe, 2020, 32, .	5.5	8
97	Composite solid electrolyte with Li ⁺ conducting 3D porous garnet-type framework for all-solid-state lithium batteries. Materials Chemistry Frontiers, 2022, 6, 1672-1680.	5.9	8
98	Comparison and evaluation of supercritical <scp> CO ₂ </scp> cooling performance in horizontal tubes with variable crossâ€section by field synergy theory. International Journal of Energy Research, 2022, 46, 14133-14144.	4.5	8
99	Electrochemical formal [3 + 2] cycloaddition of azobenzenes with hexahydro-1,3,5-triazines. Organic Chemistry Frontiers, 2022, 9, 3769-3774.	4.5	8
100	Enantioselective Synthesis of Highly Substituted Chromans by a Zinc(II)-Catalyzed Tandem Friedel-Crafts Alkylation/Michael Addition Reaction. Synthesis, 2013, 45, 601-608.	2.3	7
101	Physicochemical and Biological Effects on Activated Sludge Performance and Activity Recovery of Damaged Sludge by Exposure to CeO2 Nanoparticles in Sequencing Batch Reactors. International Journal of Environmental Research and Public Health, 2019, 16, 4029.	2.6	7
102	Comparison analysis on simultaneous decolorization of Congo red and electricity generation in microbial fuel cell (MFC) with l-threonine-/conductive polymer-modified anodes. Environmental Science and Pollution Research, 2021, 28, 4262-4275.	5.3	7
103	Gastrin-17 induces gastric cancer cell epithelial-mesenchymal transition via the Wnt/β-catenin signaling pathway. Journal of Physiology and Biochemistry, 2021, 77, 93-104.	3.0	7
104	Catalytic ozonation of dibutyl phthalate in the presence of Ag-doped NiFe ₂ O ₄ and its mechanism. Environmental Technology (United Kingdom), 2021, 42, 4528-4538.	2.2	7
105	Improving the Estimation of Human Climate Influence by Selecting Appropriate Forcing Simulations. Geophysical Research Letters, 2021, 48, e2021GL095500.	4.0	7
106	Selection and Validation of Reference Genes for RT-qPCR Normalization in Bradysia odoriphaga (Diptera: Sciaridae) Under Insecticides Stress. Frontiers in Physiology, 2021, 12, 818210.	2.8	7
107	Spectral characterization of fiber Bragg grating with etched fiber cladding. Optoelectronics Letters, 2012, 8, 328-331.	0.8	6
108	Solvothermal synthesis of wire-like SnxSb2Te3+x with an enhanced thermoelectric performance. Dalton Transactions, 2016, 45, 7483-7491.	3.3	6

#	Article	IF	CITATIONS
109	Role of indium tin oxide electrode on the microstructure of self-assembled WO3-BiVO4 hetero nanostructures. Journal of Applied Physics, 2017, 122, .	2.5	6
110	On the Optimal Design of Field Significance Tests for Changes in Climate Extremes. Geophysical Research Letters, 2021, 48, e2021GL092831.	4.0	6
111	Response of metabolic and lipid synthesis gene expression changes in Camellia oleifera to mulched ecological mat under drought conditions. Science of the Total Environment, 2021, 795, 148856.	8.0	6
112	Temperature-insensitive fiber Bragg grating strain sensor. Optoelectronics Letters, 2012, 8, 414-417.	0.8	5
113	Microstructure of Cu2S nanoprecipitates and its effect on electrical and thermal properties in thermoelectric Cu2Zn0.2Sn0.8S3 ceramics. AIP Advances, 2018, 8, 085105.	1.3	5
114	Fabrication of carbohydrate microarrays on poly(2-hydroxyethyl methacrylate)-cyanuric chloride-modified substrates for the analysis of carbohydrate–lectin interactions. New Journal of Chemistry, 2019, 43, 9145-9151.	2.8	5
115	Anthropogenic influence on the intensity of extreme precipitation in the <scp>Asianâ€Australian</scp> monsoon region in <scp>HadGEM3â€Aâ€N216</scp> . Atmospheric Science Letters, 2021, 22, e1036.	1.9	5
116	Chromium-Catalyzed Borylative Coupling of Aliphatic Bromides with Pinacolborane by Hydrogen Evolution. Organometallics, 2021, 40, 2204-2208.	2.3	5
117	Emerging Global Ocean Deoxygenation Across the 21st Century. Geophysical Research Letters, 2021, 48, e2021GL095370.	4.0	5
118	Non-uniform changes in different daily precipitation events in the contiguous United States. Weather and Climate Extremes, 2022, 35, 100417.	4.1	5
119	Chromium-Catalyzed Selective Borylation of Vinyl Triflates and Unactivated Aryl Carboxylic Esters with Pinacolborane. Organic Letters, 2022, 24, 3227-3231.	4.6	5
120	Paleoecology of Early Ordovician Reefs in the Yichang Area, Hubei: a Correlation of Organic Reefs Between Early Ordovician and Jurassic. Acta Geologica Sinica, 2011, 85, 1003-1015.	1.4	4
121	Novel method to integrate MARG and an odometer into AHRS for moving vehicles. Advances in Mechanical Engineering, 2017, 9, 168781401772797.	1.6	4
122	Microstructure evolution determined by the crystalline phases competition in self-assembled WO3-BiVO4 hetero nanostructures. Journal of Applied Physics, 2018, 123, 085305.	2.5	4
123	Evolution of cation ordering and crystal defects controlled by Zn substitutions in Cu2SnS3 ceramics. AIP Advances, 2018, 8, 105322.	1.3	4
124	Sediment Routing and Anthropogenic Impact in the Huanghe River Catchment, China: An Investigation Using Nd Isotopes of River Sediments. Water Resources Research, 2021, 57, e2020WR028444.	4.2	4
125	The January 2021 Cold Air Outbreak over Eastern China: Is There a Human Fingerprint?. Bulletin of the American Meteorological Society, 2022, 103, S50-S54.	3.3	4
126	Chromium-catalyzed couplings of C(aryl)–SMe bonds for accessing arylated and alkylated benzaldehyde derivatives. Chemical Communications, 2022, 58, 7094-7097.	4.1	4

#	Article	IF	CITATIONS
127	Nonlocality distillation for high-dimensional correlated boxes. Quantum Information Processing, 2015, 14, 1321-1331.	2.2	3
128	Operational and biological analyses of branched water-adjustment and combined treatment of wastewater from a chemical industrial park. Environmental Technology (United Kingdom), 2018, 39, 253-263.	2.2	3
129	Modeling of instantaneous cutting force for large pitch screw with vibration consideration of the machine tool. International Journal of Advanced Manufacturing Technology, 2020, 108, 3893-3904.	3.0	3
130	Effect of electric potentials on the removal of Cu and Zn in soil by electrokinetic remediation. Separation Science and Technology, 2021, 56, 2439-2448.	2.5	3
131	Bioinformatics analysis for the identification of differentially expressed genes and related signaling pathways in <i>H. pylori-</i> CagA transfected gastric cancer cells. PeerJ, 2021, 9, e11203.	2.0	3
132	Practical Synthesis of (<i>Z</i>)-α,β-Unsaturated Nitriles via a One-Pot Sequential Hydroformylation/Knoevenagel Reaction. Journal of Organic Chemistry, 2021, 86, 15413-15422.	3.2	3
133	A low-cost and effective seeding technique using protective core for restoration of <i>Zostera marina</i> habitats. Aquatic Ecosystem Health and Management, 2020, 23, 341-349.	0.6	3
134	Operator Entanglement of Two-Qubit Joint Unitary Operations Revisited: Schmidt Number Approach. Brazilian Journal of Physics, 2012, 42, 167-171.	1.4	1
135	Stability and economy analysis based on computational fluid dynamics and field testing of hybrid-driven underwater glider with the water quality sensor in Danjiangkou Reservoir. Advances in Mechanical Engineering, 2015, 7, 168781401562057.	1.6	1
136	Carbohydrate microarray-based analysis of specific interactions between saccharides from algin and influenza A viral hemagglutinin. Analytical Methods, 2019, 11, 3641-3647.	2.7	1
137	Paleoecology of Early Ordovician Reefs in the Yichang Area, Hubei: a Correlation of Organic Reefs Between Early Ordovician and Jurassic. Acta Geologica Sinica, 2011, 85, 1003-1015.	1.4	1
138	Spatial effects on extreme precipitation in the coastal areas of southeastern China during the raining season. International Journal of Climatology, 0, , .	3.5	1
139	Research on Approach of Entropy-Based Wavelet Filtering for Nomadic Service. , 2009, , .		0
140	Passive wireless pressure sensor fabricated in low-temperature co-fired ceramic technology. Proceedings of the Institution of Mechanical Engineers, Part N: Journal of Nanoengineering and Nanosystems, 2015, 229, 160-165.	0.1	0
141	Geochemistry and provenances of core sediments from the Shikoku Basin. Geological Journal, 2016, 51, 60-76.	1.3	0
142	Simultaneous nitrification and denitrification via nitrite in a pilot-scale modified anaerobic-anoxic-oxic reactor. Desalination and Water Treatment, 2016, 57, 19609-19618.	1.0	0
143	Circuit Optimization of the HTS Transformer-rectifier Flux Pump. , 2020, , .		0